Supporting Information

Dominant driving forces in human telomere quadruplex binding-induced structural alterations

Matjaz Boncina,[1] Florian Hamon,[2] Barira Islam,[3] Marie-Paule Teulade-Fichou,[2] Gorazd Vesnaver,[1] Shozeb Haider,[3,4] and Jurij Lah[1,*]

[1]Faculty of Chemistry and Chemical Technology, University of Ljubljana, Večna pot 113, SI–1000 Ljubljana, Slovenia.

[2]Institut Curie, CNRS UMR-176, Centre Universitaire d'Orsay, Paris-Sud 91405 Orsay Cedex France.

[3]Centre for Cancer Research and Cell Biology, Queen's University of Belfast, Belfast BT9 7BL, UK.

[4]UCL School of Pharmacy 29-39 Brunswick Square, Bloomsbury, London WC1N 1AX, UK.

*Corresponding author footnote:
Jurij Lah
Faculty of Chemistry and Chemical Technology, University of Ljubljana, SI–1000 Ljubljana, Slovenia.
E-mail: jurij.lah@fkkt.uni-lj.si

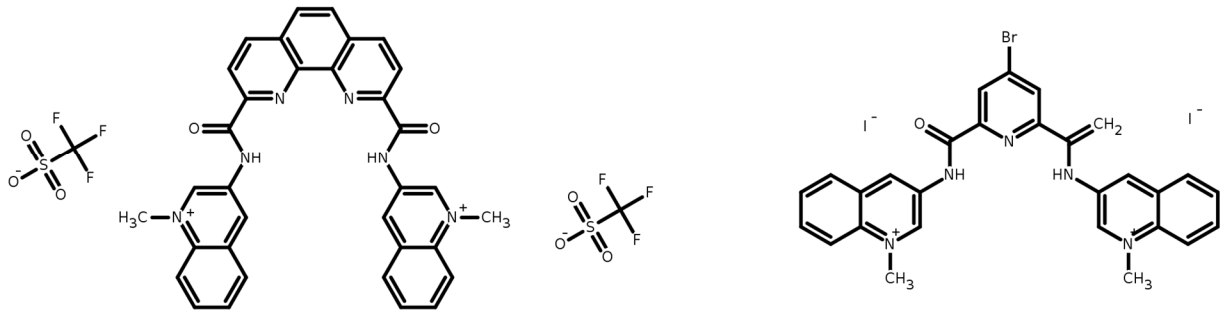

FIGURE S1 Bisquinolinium ligands used in this study: The Phenanthroline Dicarboxamide derivative Phen-DC3 (left), and the Bromo-Pyridine Dicarboxamide derivative 360A-Br.

METHODS

Model Based Analysis of Experimental Data

The simplest model mechanism of ion and ligand binding-coupled folding of Tel22, that successfully describes the corresponding calorimetric and spectroscopic data obtained in solutions with K^+ or Na^+, ions involves five macroscopic states: U (unfolded DNA), I (intermediate), Q (folded G-quadruplex), Q'L and Q''L_2 (folded G-quadruplex with one and two bound ligand molecules).

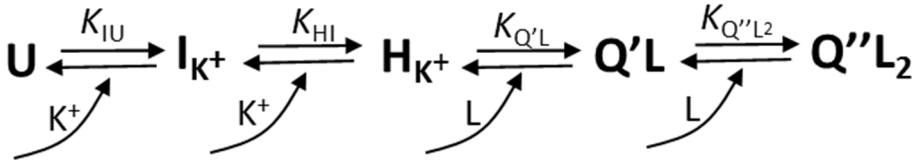

FIGURE S2 Schematic presentation of the simplest equilibrium model of ion- and ligand (L)-induced Tel22 structural transitions in the presence of K^+ ions (see also Scheme 1 in the main text) that at various temperatures and salt concentrations assumes inter-conversions between the unfolded (U), the intermediate (I), the folded G-quadruplex structure (Q), and the quadruplex complexes with one or two bound ligand molecules (Q'L, Q''L_2).

For a given model one can write a general equation for the measured spectroscopic and calorimetric properties of the ion-ligand-DNA solution (Eq.1) from which the corresponding contributions of the buffer are subtracted. Such property, *X*, can be presented as a linear

combination of molar ratios, $\alpha_j = [c_j]/c_{DNA}$ of all species, j, present in the solution (j = L, U, I, Q, Q'L, Q''L_2)

$$X = X_L\alpha_L + X_U\alpha_U + X_I\alpha_I + X_Q\alpha_Q + X_{Q'L}\alpha_{Q'L} + X_{Q''L_2}\alpha_{Q''L_2} \quad (1)$$

where X_j represents the property of the solute j at a given pressure, P, temperature, T, salt type (KCl, NaCl), salt concentration and the total DNA concentration, c_{DNA}. Since according to the model $\alpha_U + \alpha_I + \alpha_Q + \alpha_{Q'L} + \alpha_{Q''L_2} = 1$ and $\alpha_L + \alpha_{Q'L} + 2\alpha_{Q''L_2} = r$ where $r = c_{L,tot} / c_{DNA} = n_{L,tot} / n_{DNA}$ ($c_{L,tot}$ is the total ligand concentration) one obtains

$$X = X_L r + (\Delta X_{IU} + \Delta X_{QI})\alpha_U + \Delta X_{QI}\alpha_I + X_Q + \Delta X_{Q'L}\alpha_{Q'L} + (\Delta X_{Q'L} + \Delta X_{Q''L_2})\alpha_{Q''L_2} \quad (2)$$

where the changes $\Delta X_{IU} = X_U - X_I$, $\Delta X_{QI} = X_I - X_Q$, $\Delta X_{Q'L} = X_{Q'L} - X_Q - X_L$, $\Delta X_{Q''L_2} = X_{Q''L_2} - X_{Q'L} - X_L$ refer to each step in the model mechanism (Fig. S2).

Unfolding/folding of Human Telomeric DNA in the Absence of Ligand

Folding/unfolding process [U ↔ I ↔ Q] of Tel22, in the presence of Na^+ or K^+ ions (no ligand present) was studied using differential scanning calorimetry (DSC) and CD spectroscopy. Experimental data obtained for Tel22 in KCl and NaCl solutions were analyzed using the three-state equilibrium model (1). In the DSC experiments the measured quantity is the partial molar heat capacity of DNA, $\overline{C}_{P,DNA}$. In the further analysis $\overline{C}_{P,DNA}$ is more conveniently expressed as the excess heat capacity, $\Delta C_P = \overline{C}_{P,DNA} - \overline{C}_{P,int}$ where $\overline{C}_{P,int}$ represents an intrinsic heat capacity of DNA formally defined as $\overline{C}_{P,int} = \alpha_Q\overline{C}_{P,Q} + \alpha_I\overline{C}_{P,I} + \alpha_U\overline{C}_{P,U}$. In the measured temperature interval, $\overline{C}_{P,int}$ was approximated by the second order polynomial on T, fitted to the low-temperature (folded form) and high-temperature (unfolded form) parts of the experimental $\overline{C}_{P,DNA}$, and then subtracted from $\overline{C}_{P,DNA}$ to obtain ΔC_P. This approach has already been described in detail in SI of ref 1. The excess heat capacity, ΔC_P, determined by DSC can also be calculated for the suggested model

from the temperature derivative of Eq. 2 for $X = H$ at constant pressure P. Since all experiments were performed at very low concentrations where $\Delta C_{P,\mathrm{ij}} = \Delta C^{\circ}_{P,\mathrm{ij}}$ and $\Delta H_{\mathrm{ij}} = \Delta H^{\circ}_{\mathrm{ij}}$ one obtains

$$\Delta C^{\circ}_{P} = (\partial \alpha_{\mathrm{U}} / \partial T)(\Delta H^{\circ}_{\mathrm{IU}} + \Delta H^{\circ}_{\mathrm{QI}}) + (\partial \alpha_{\mathrm{I}} / \partial T)\Delta H^{\circ}_{\mathrm{QI}} \tag{3}$$

where $\Delta H^{\circ}_{\mathrm{IU}}$ and $\Delta H^{\circ}_{\mathrm{QI}}$ are the standard enthalpies of I → U and Q → I transition, respectively. The measured CD spectra may be described in a similar way. In this case the quantity X in Eq. 1 represents, [Θ], that is the measured ellipticity at a given wavelength, Θ, divided by the optical path length, l, and the total DNA concentration, c_{DNA}. By taking into account that the molar ellipticities of G-quadruplex in the folded, $[\Theta]_{\mathrm{Q}}$, and unfolded, $[\Theta]_{\mathrm{U}}$, state can be obtained by extrapolation of [Θ] from pre-, $[\Theta]_{\mathrm{Q}}$, and post-, $[\Theta]_{\mathrm{U}}$, transitional parts of the unfolding curves and that $\alpha_{\mathrm{Q}} = 1 - \alpha_{\mathrm{I}} - \alpha_{\mathrm{U}}$ one can express the experimentally obtained induced signal f in terms of the model function (1).

$$f = \frac{[\Theta] - [\Theta]_{\mathrm{Q}}}{[\Theta]_{\mathrm{U}} - [\Theta]_{\mathrm{Q}}} = \alpha_{\mathrm{I}} f_{\mathrm{QI}} + \alpha_{\mathrm{U}} \tag{4}$$

in which f_{QI} can be considered as the temperature independent normalization coefficient.

Binding of the Ligands to Human Telomeric DNA

In order to study binding of the selected ligands to Tel22 in buffer solutions we have to make sure that the ligands are soluble and that the formed ligand-DNA complexes do no aggregate. These problems were overcome by dissolving the ligands in buffer solution containing 3% DMSO and by titrating DNA solution containing 3% DMSO into the ligand solution. The choice of DMSO was based on the experimental evidence that up to 5% DMSO has practically no effect on the thermodynamic quantities of binding (2,3). The ligand binding experiments were performed at conditions (T, salt concentration) where only intermediate (I) and folded G-quadruplex (Q) conformations were present at the beginning of the experiment, but not the unfolded DNA ($\alpha_{\mathrm{U}} = 0$).

In the case of CD titrations the quantity X in Eq. 2 is at any titration point presented as [Θ], that is the measured ellipticity, Θ, at a given wavelength divided by the optical path length, l, and the total DNA concentration, c_{DNA}. By subtracting molar ellipticity of the folded G-quadruplex, $[\Theta]_Q$, and taking into account that the unbound ligands are not optically active ($[\Theta]_L = 0$) one obtains a relation between the experimentally obtained induced signal Δ[Θ] (left-hand side of Eq. 5) and the model function (right-hand side of Eq. 5)

$$\Delta[\Theta] = [\Theta] - [\Theta]_Q = \Delta[\Theta]_{QI}\,\alpha_I + \Delta[\Theta]_{Q'L}\,\alpha_{Q'L} + \left(\Delta[\Theta]_{Q'L} + \Delta[\Theta]_{Q''L_2}\right)\alpha_{Q''L_2} \tag{5}$$

Similarly, in the case of fluorimetry the quantity X in Eq. 2 represents normalized measured emitted fluorescence, $X=[F]=I_F/(c_{DNA}l)$. By subtracting the normalized fluorescence that ligand would have at the same total ligand concentration in the absence of DNA, $[F]_L \cdot r$, and by taking into account that DNA itself does not emit fluorescence ($[F]_Q = 0$, $\Delta[F]_{QI} = 0$) one obtains

$$\Delta[F] = [F] - [F]_L\, r = \Delta[F]_{Q'L}\,\alpha_{Q'L} + \left(\Delta[F]_{Q'L} + \Delta[F]_{Q''L_2}\right)\alpha_{Q''L_2} \tag{6}$$

In the case of ITC, the quantity X in Eq. 2 represents H_m, that is, the enthalpy of solution in the measuring cell expressed per mole of DNA from which the corresponding enthalpy of solvent S (buffer solution) is subtracted

$$H_m = \bar{H}_L r + \Delta H_{QI}\alpha_I + \bar{H}_Q + \Delta H_{Q'L}\alpha_{Q'L} + \left(\Delta H_{Q'L} + \Delta H_{Q''L_2}\right)\alpha_{Q''L_2} \tag{7}$$

$\bar{H}_L$ and $\bar{H}_Q$ are the partial molar enthalpies of ligand and the folded G-quadruplex, and ΔH_{QI}, $\Delta H_{Q'L}$ and $\Delta H_{Q''L_2}$ are the enthalpies of Q → I, Q → Q'L and Q'L → Q''L_2 transitions, respectively. By multiplying Eq. 7 with the total amount of the DNA, n_{DNA}, taking the partial derivative of this expression with respect to n_{DNA} at P, T, n_S, $n_{L,tot}$ = const. and using the Gibbs-Duhem relation one

obtains an expression for the partial molar enthalpy of the DNA, $\bar{H}_{\mathrm{DNA}}$, which at very low concentrations, where $\bar{H}_{\mathrm{i}} = \bar{H}_{\mathrm{i}}^{\mathrm{o}}$ and $\bar{H}_{\mathrm{ij}} = \bar{H}_{ij}^{\mathrm{o}}$, becomes

$$\bar{H}_{\mathrm{DNA}} = \Delta H_{\mathrm{QI}}^{\mathrm{o}} \left(\partial n_{\mathrm{I}} / \partial n_{\mathrm{DNA}}\right)_{P,T,n_{\mathrm{S}},n_{\mathrm{L,tot}}} + \bar{H}_{\mathrm{Q}}^{\mathrm{o}} + \Delta H_{\mathrm{Q'L}}^{\mathrm{o}} \left(\partial n_{\mathrm{Q'L}} / \partial n_{\mathrm{DNA}}\right)_{P,T,n_{\mathrm{S}},n_{\mathrm{L,tot}}} + \left(\Delta H_{\mathrm{Q'L}}^{\mathrm{o}} + \Delta H_{\mathrm{Q''L_2}}^{\mathrm{o}}\right)\left(\partial n_{\mathrm{Q''L_2}} / \partial n_{\mathrm{DNA}}\right)_{P,T,n_{\mathrm{S}},n_{\mathrm{L,tot}}} \tag{8}$$

Each $(\partial n_{\mathrm{j}} / \partial n_{\mathrm{DNA}})$ term (j = I, Q'L, Q''L_2) in Eq. 8 represents the corresponding partial derivative at n_{DNA} at P, T, n_{S}, $n_{\mathrm{L,tot}}$ = const. which can be further expressed analytically in terms of α_{j} ($\alpha_{\mathrm{j}} = n_{\mathrm{j}}/n_{\mathrm{DNA}}$). In order to obtain enthalpy changes resulting from complex formation, ΔH_T, one needs to perform the blank titration experiment, that is the titration of DNA into the ligand free buffer solution. From Eq. 8 we obtain $\left(\bar{H}_{\mathrm{DNA}}\right)_{\mathrm{bl}} = \Delta H_{\mathrm{QI}}^{\mathrm{o}} \left(\partial n_{\mathrm{I}} / \partial n_{\mathrm{DNA}}\right) + \bar{H}_{\mathrm{Q}}^{\mathrm{o}}$ at P, T, n_{S}, $n_{\mathrm{L=0}}$ = const. and by subtracting this expression from Eq. 8 one obtains the quantity of interest, ΔH_T

$$\begin{aligned}\Delta H_T = \bar{H}_{\mathrm{DNA}} - \left(\bar{H}_{\mathrm{DNA}}\right)_{\mathrm{bl}} = \Delta H_{\mathrm{Q'L}}^{\mathrm{o}} \left(\partial n_{\mathrm{Q'L}} / \partial n_{\mathrm{DNA}}\right)_{P,T,n_{\mathrm{S}},n_{\mathrm{L,tot}}} + \left(\Delta H_{\mathrm{Q'L}}^{\mathrm{o}} + \Delta H_{\mathrm{Q''L_2}}^{\mathrm{o}}\right)\left(\partial n_{\mathrm{Q''L_2}} / \partial n_{\mathrm{DNA}}\right)_{P,T,n_{\mathrm{S}},n_{\mathrm{L,tot}}} \\ + \Delta H_{\mathrm{QI}}^{\mathrm{o}} \left(\left(\partial n_{\mathrm{I}} / \partial n_{\mathrm{DNA}}\right)_{P,T,n_{\mathrm{S}},n_{\mathrm{L,tot}}} - \left(\partial n_{\mathrm{I}} / \partial n_{\mathrm{DNA}}\right)_{P,T,n_{\mathrm{S}},n_{\mathrm{L=0}}}\right)\end{aligned} \tag{9}$$

Global Model Analysis of Experimental Data

Model functions (Eqs. 3-6, 9) resulting from the suggested model (Figure S2, Scheme 1 – main text) were used to describe CD, FL, ITC and DSC data as presented in the main text on page 6.

RESULTS

The "best fit" thermodynamic parameters describing folding/unfolding of Tel22 in the presence of K^+ and Na^+ ions at T_0 = 298.15 K obtained by the semi-global analysis of DSC and CD data (Eqs. 3, 4) are presented in Table S1 and Fig. S3.

As already mentioned, ligands were dissolved in buffer solution containing 3% DMSO, therefore also DNA was prepared in the same solution. In order to examine the effect of DMSO on thermodynamics of folding/unfolding of Tel22 we performed a series of DSC and CD experiments in pure aqueous and 3% DMSO solutions in the presence of K^+ ions (100 mM KCl)

and globally analyzed them with the same model. The comparison of results obtained for both types of solutions clearly shows that the presence of 3 % of DMSO in aqueous solutions has negligible effect on the thermodynamics of Tel22 folding/unfolding processes. Consequently, for description of thermodynamics of folding/unfolding of Tel22 in 3% DMSO solutions in the presence of 100 mM or 200 mM NaCl or KCl the corresponding thermodynamic parameters obtained in DMSO free aqueous solutions were used.

TABLE S1 The "best fit" thermodynamic parameters accompanying folding of Tel22 in Na^+ and K^+ solutions in the absence of ligand at T_0 = 25 °C K obtained by the global three-state model (Eqs. 3, 4) analysis of DSC and CD data.

	100 mM Na^+		100 mM K^+	
	U → I	I → Q	U → I	I → Q
$\Delta G^{o}_{T_0,X^+}$ / kcal mol^{-1}	-3.1±0.1	-0.7±0.1	-3.7±0.1	-1.4±0.1
$\Delta H^{o}_{T_0}$ / kcal mol^{-1}	-25.4±1.0	-20.1±0.2	-23.6±0.6	-22.4±0.1
$T\Delta S^{o}_{T_0,X^+}$ / kcal mol^{-1}	-22.3±1.0	-19.4±0.2	-19.9±0.6	-21.0±0.1
ΔC^{o}_{P} / cal mol^{-1} K^{-1}	-390±30	0±10	-420±20	0±20

Errors represent 2x standard deviations obtained as square roots of diagonal elements of the corresponding variance-covariance matrixes. For comparative purposes $\Delta G^{o}_{T_0}$ was extrapolated from [X^+] = 1 M (best fit parameter value) to [X^+] = 100 mM (this table) by using Eq. 3 – main text.

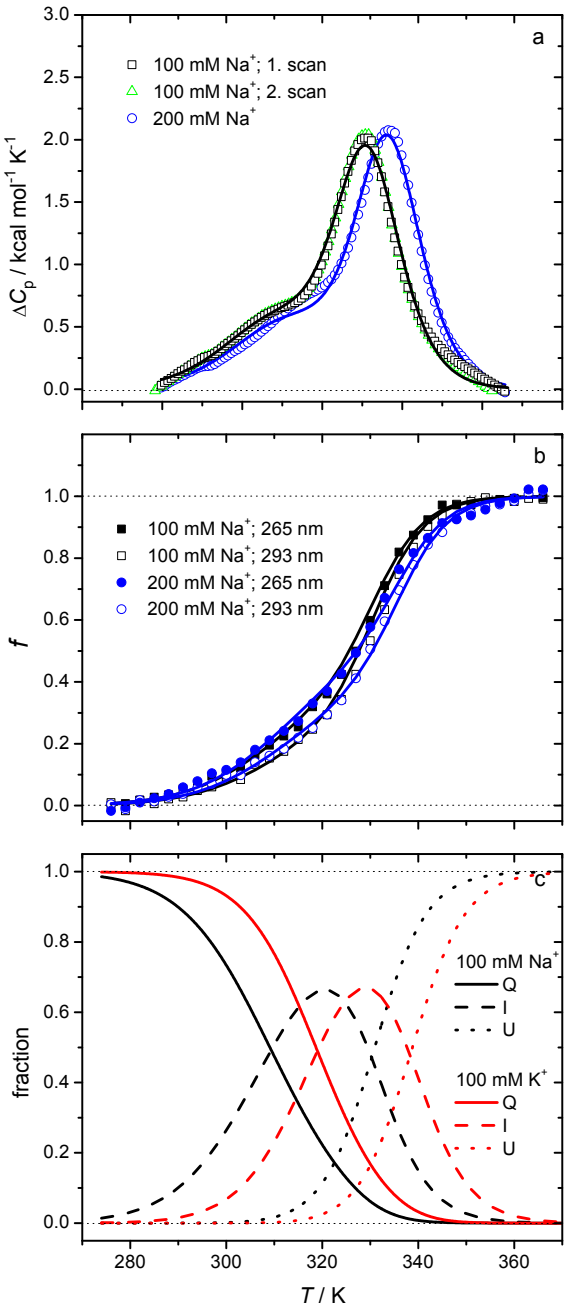

FIGURE S3 Global analysis of the DSC thermograms and CD melting curves measured at different concentrations of Na^+ ions in cacodylic buffer, pH = 6.9, in the absence of ligand.

a) DSC thermograms of Tel22 at different Na^+ concentrations. Experimental data are presented by symbols while the lines refer to the corresponding best global fit of the model function (Eq. 3). DSC thermograms are reproducible in the presence of Na^+ or K^+ (typical 1. and 2. scan for Na^+ are presented) suggesting that folding/unfolding of Tel22 in the presence of ions may be considered as a reversible process. For clarity reasons only every 10th experimental point is shown.

b) Normalized CD melting curves at 265 and 293 nm. Experimental data are presented by symbols while the corresponding best global fit of the model function (Eq. 4) is presented by the lines.

c) The model-predicted fractions of species Q, I and U as a function of *T* in 100 mM Na^+ and 100 mM K^+ determined using the "best fit" parameters reported in Table S1.

TABLE S2 The "best fit" thermodynamic parameters describing binding of Phen-DC3 and 360A-Br to Tel22 at T_0 = 25 °C in the presence of 100 mM Na^+ or 100 mM K^+ ions obtained from global fitting of the model functions (Eqs. 5, 6, 9) to the CD, FL and ITC data presented in Figs. S4-S7.

	Phen-DC3		360A-Br	
	100 mM Na^+	100 mM K^+	100 mM Na^+	100 mM K^+
$K_{Q'L}$	$8.8\cdot10^6$	$5.5\cdot10^6$	$5.3\cdot10^6$	$3.2\cdot10^6$
$\Delta G^o_{Q'L(T_0,X^+)}$ / kcal mol^{-1}	-9.5±0.4	-9.2±0.4	-9.2±0.4	-8.9±0.4
$\Delta H^o_{Q'L(T_0)}$ / kcal mol^{-1}	-13.1±0.4	-13.6±0.4	-15.1±0.6	-15.0±0.6
$T_0\Delta S^o_{Q'L(T_0,X^+)}$ / kcal mol^{-1}	-3.6±0.6	-4.4±0.6	-5.9±0.7	-6.1±0.7
$K_{Q''L_2}$	$3.3\cdot10^6$	$2.2\cdot10^6$	$1.6\cdot10^6$	$6.1\cdot10^5$
$\Delta G^o_{Q''L_2(T_0,X^+)}$ / kcal mol^{-1}	-8.9±0.4	-8.7±0.4	-8.5±0.4	-7.9±0.4
$\Delta H^o_{Q''L_2(T_0)}$ / kcal mol^{-1}	-11.3±0.4	-9.8±0.4	-16.4±0.6	-17.2±0.6
$T_0\Delta S^o_{Q''L_2(T_0,X^+)}$ / kcal mol^{-1}	-2.4±0.6	-1.2±0.6	-7.9±0.7	-9.3±0.7
$\Delta C^o_{P,Q'L} = \Delta C^o_{P,Q''L_2}$ / cal mol^{-1} K^{-1}	-510±60	-540±60	-400±60	-300±60
$\Delta n_{Q'L} = \Delta n_{Q''L_2}$	1.3±0.4	1.5±0.2	1.2±0.2	1.2±0.2
	U → Q'L	U → Q'L	U → Q'L	U → Q'L
$\Delta G^o_{i(T_0,X^+)}$ / kcal mol^{-1}	-13.3±0.4	-14.3±0.4	-13.0±0.4	-14.0±0.4
$\Delta H^o_{i(T_0,X^+)}$ / kcal mol^{-1}	-58.6±1.0	-59.6±0.7	-60.6±1.2	-61.0±0.8
$T_0\Delta S^o_{i(T_0,X^+)}$ / kcal mol^{-1}	-45.3±1.1	-45.3±0.9	-47.6±1.3	-47.0±0.9
	U → Q''L_2	U → Q''L_2	U → Q''L_2	U → Q''L_2
$\Delta G^o_{i(T_0,X^+)}$ / kcal mol^{-1}	-22.2±0.6	-23.0±0.6	-21.5±0.6	-21.9±0.6
$\Delta H^o_{i(T_0,X^+)}$ / kcal mol^{-1}	-69.9±1.1	-69.4.0±0.8	-77.0±1.3	-78.2±1.0
$T_0\Delta S^o_{i(T_0,X^+)}$ / kcal mol^{-1}	-47.6±1.3	-46.4±1.0	-55.5±1.4	-56.3±1.2

Errors represent 2x standard deviations obtained as square roots of diagonal elements of the corresponding variance-covariance matrixes.

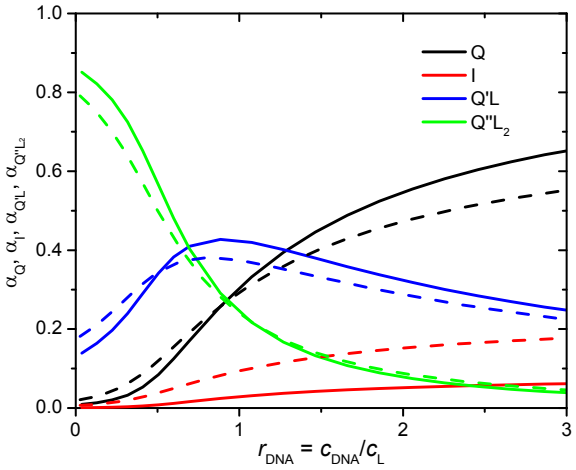

FIGURE S4 Binding of Phen-DC3 on Tel22 in the presence of K^+ ions. The model-predicted fractions of species Q, I, Q'L and Q''L_2 at 25 (solid lines) and 35 (dashed lines) °C and 100 mM K^+ as a function of molar ratio $r_{DNA} = c_{DNA}/c_L$ determined using the "best fit" parameters reported in Table S2.

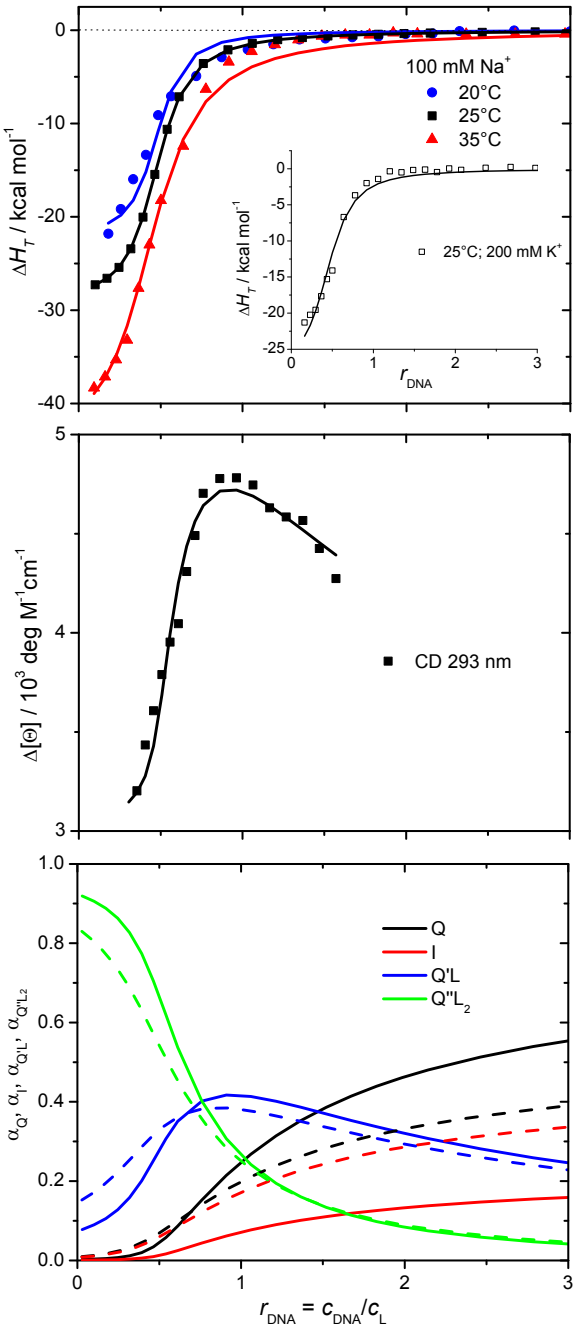

FIGURE S5 Binding of Phen-DC3 on Tel22 in the presence of Na^+ ions. Global analysis of the ITC and CD binding data measured at different *T* and different concentrations of Na^+ ions. Experimental ITC data are presented by symbols, while the lines refer to the corresponding best global fit of the model function (Eq. 9).

Experimental CD-titration data measured at 25°C in the presence of 100 mM Na^+ ions are presented by symbols while the corresponding best global fit of the model function (Eq. 5) is presented by the line.

The model-predicted fractions of species Q, I, Q'L and Q''L_2 at 25 (solid lines) and 35 (dashed lines) °C and 100 mM Na^+ as a function of molar ratio $r_{DNA} = c_{DNA}/c_L$ determined using the "best fit" parameters reported in Table S2.

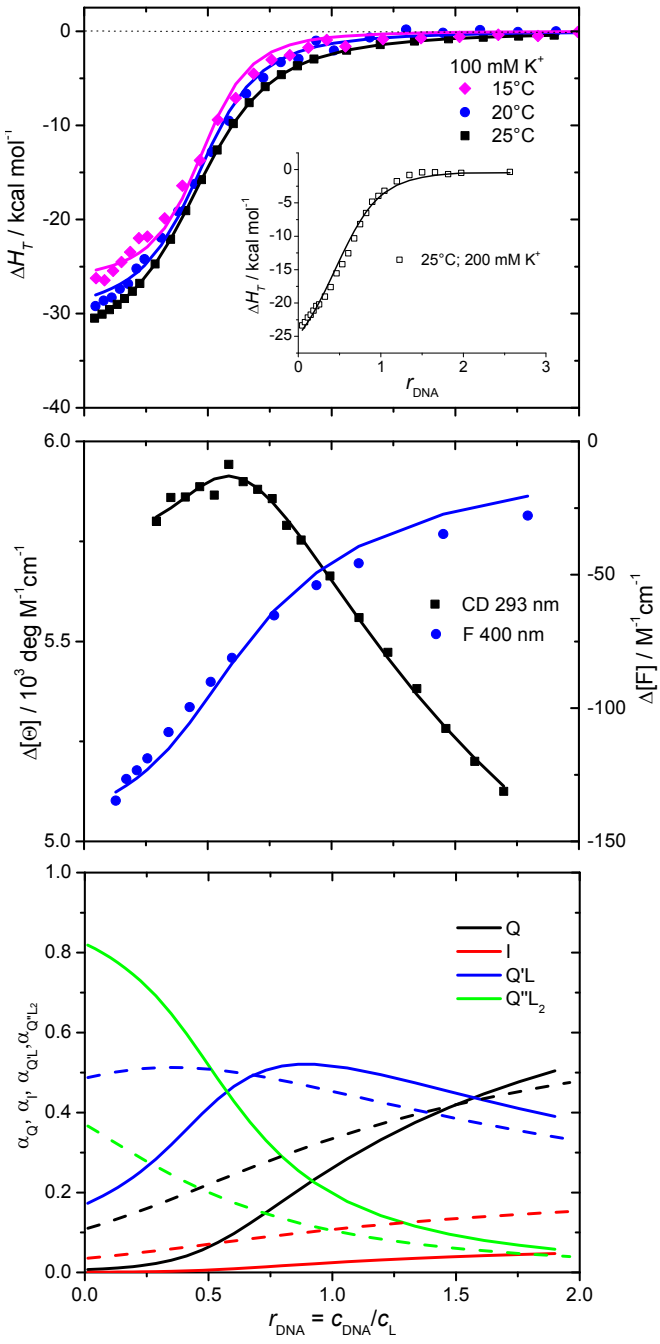

FIGURE S6 Binding of 360A-Br on Tel22 in the presence of K^+ ions. Global analysis of the ITC, CD and FL binding data measured at different *T* and different concentrations of K^+ ions. Experimental ITC data are presented by symbols, while the lines refer to the corresponding best global fit of the model function (Eq. 9).

Experimental CD- and FL-titration data measured at 25°C in the presence of 100 mM K^+ ions are presented by symbols while the corresponding best global fit of the model function (Eqs. 5 and 6) is presented by the lines.

The model-predicted fractions of species Q, I, Q'L and Q''L_2 at 25 (solid lines) and 35 (dashed lines) °C and 100 mM K^+ as a function of molar ratio $r_{DNA} = c_{DNA}/c_L$ determined using the "best fit" parameters reported in Table S2.

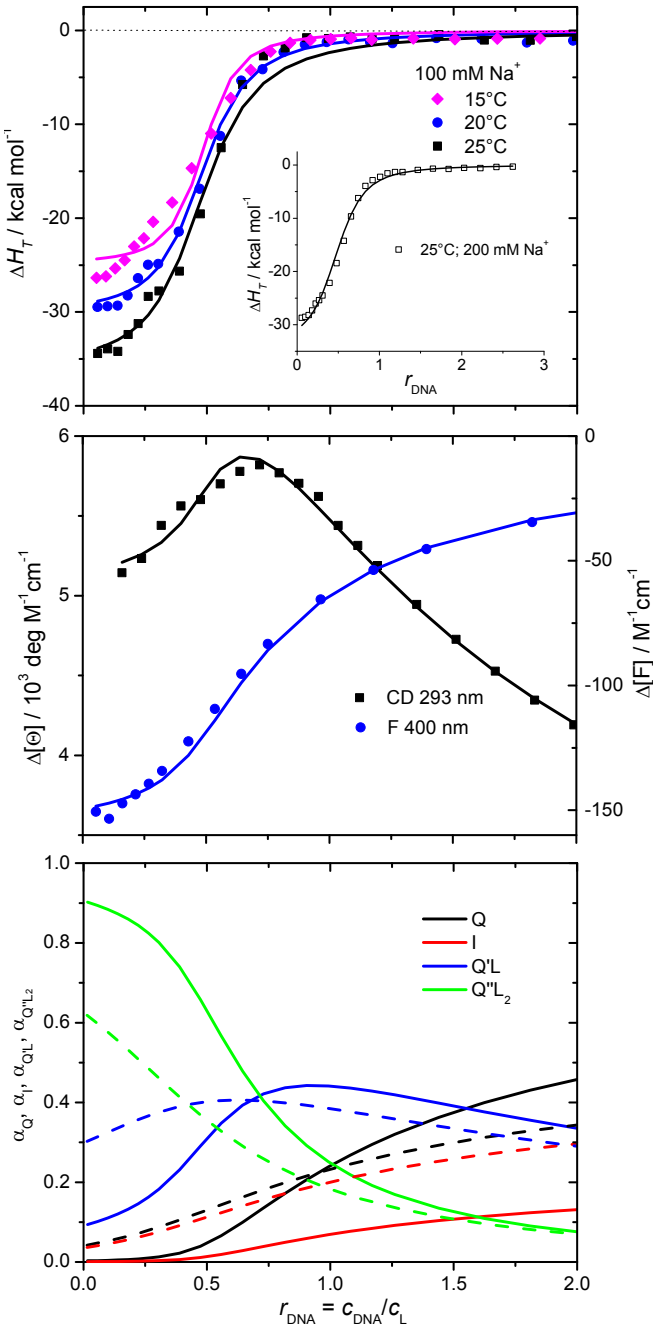

FIGURE S7 Binding of 360A-Br on Tel22 in the presence of Na^+ ions. Global analysis of the ITC, CD and FL binding data measured at different *T* and different concentrations of Na^+ ions. Experimental ITC data are presented by symbols, while the lines refer to the corresponding best global fit of the model function (Eq. 9).

Experimental CD- and FL-titration data measured at 25°C in the presence of 100 mM Na^+ ions are presented by symbols while the corresponding best global fit of the model function (Eqs. 5 and 6) is presented by the lines.

The model-predicted fractions of species Q, I, Q'L and Q''L_2 at 25 (solid lines) and 35 (dashed lines) °C and 100 mM Na^+ as a function of molar ratio $r_{DNA} = c_{DNA}/c_L$ determined using the "best fit" parameters reported in Table S2.

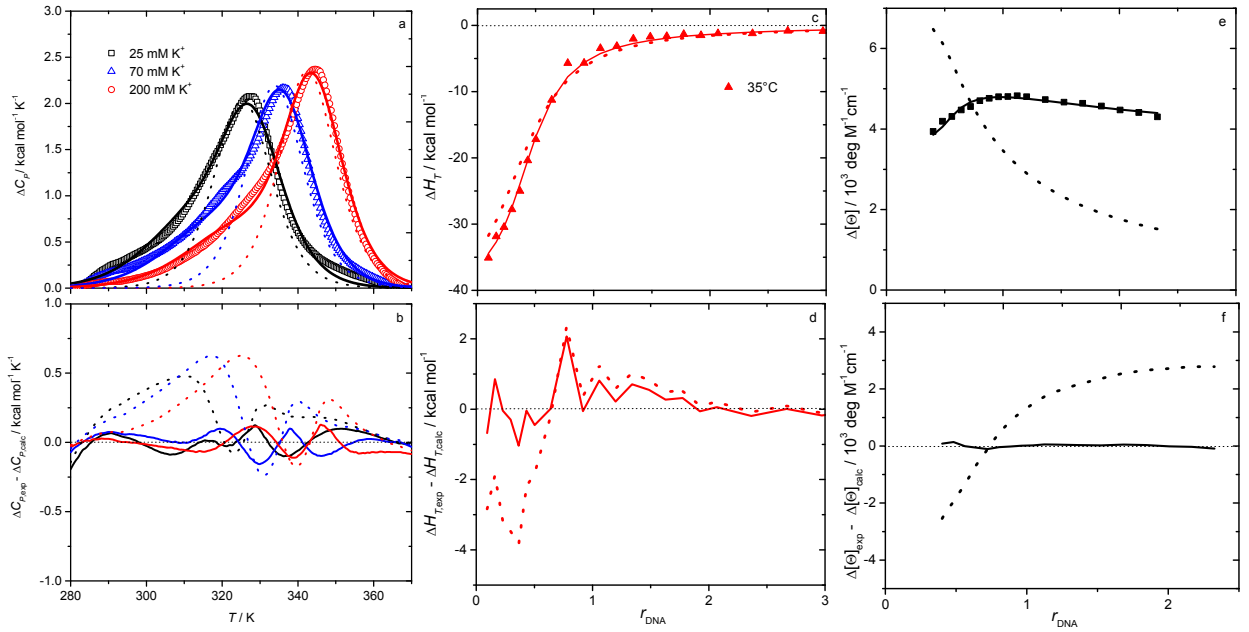

FIGURE S8 Comparison of some characteristic of global fit of the Model 1, Model 2 and Model 3 to the data presented in Fig. 1 of the main text. (a) DSC thermograms: Tel22 at different K^+ concentrations. Experimental data are presented by symbols, the solid lines refer to the corresponding best global fit of the three-state model function (U ↔ I ↔ Q + L ↔ Q'L + L ↔ Q''L_2, Model 1) and the dotted lines to the corresponding best global fit of the two-state model function (U ↔ Q+ L ↔ Q'L + L ↔ Q''L_2, Model 2) in ligand free solution. (b) Differences between experimental ΔC_P values and those calculated by the Model 1 (solid lines) or the Model 2 (dotted lines). (c) ITC titration of Phen-DC3 to Tel22 at 35 °C: Model 2 fits worse (dotted line) the measured ligand binding data (symbols) if the model predicted population of I is not taken into account (at 35 °C the population of I changes for about 20 %; see Figs. S4-S7). (d) Differences between experimental ΔH_T values (symbols) and calculated from the Model 1 (solid line) and Model 2 (dotted line) for binding of Phen-DC3 to Tel22 at 35 °C. (e) CD titration of Phen-DC3 to Tel22 at 25 °C and 293 nm: Model 3 (binding steps described in terms of two identical independent binding sites model) fits worse (dotted line) the measured ligand binding data (symbols) as Model 1 (solid line). (f) Differences between experimental Δ[θ] values (symbols) and calculated from Model 1 (solid line) and Model 3 (dotted line) for binding of Phen-DC3 to Tel22 at 25 °C.

TABLE S3 Dissection of Gibbs free energy changes (Eq. 4 – main text) for each model predicted step (Scheme 1 - main text) at 25 °C and 100 mM Na^+ or K^+ (L = Phen-DC3).

Na^+	$\Delta G°_{solv}$ / kcal mol^{-1}		$\Delta G°_{int}$ / kcal mol^{-1}	$\Delta G°_{rt}$ / kcal mol^{-1}	$\Delta G°_{conf}$ / kcal mol^{-1}
	$\Delta G°_{ion}$	$\Delta G°_{hyd}$			
U → I	90 ± 1	–31 ± 4	–123 ± 2	0	61 ± 7
I → Q	90 ± 1	0	–117 ± 2	0	27 ± 3
Q + L → Q'L	0	–41 ± 8	–11.3 ± 0.2	15 ± 3	28 ± 11
Q'L + L → Q''L_2	0	–41 ± 8	–13.1 ± 0.2	15 ± 3	30 ± 11
U + 2L → Q''L_2	179 ± 3	–113 ± 20	–265 ± 4	30 ± 6	146 ± 33
K^+					
U → I	73 ± 1	–34 ± 3	–101 ± 2	0	58 ± 6
I → Q	73 ± 1	0	–99.8 ± 2	0	26 ± 5
Q + L → Q'L	0	–43 ± 8	–13.6 ± 0.2	15 ± 3	33 ± 11
Q'L + L → Q''L_2	0	–43 ± 8	–9.8 ± 0.2	15 ± 3	29 ± 11
U + 2L → Q''L_2	145 ± 3	–120 ± 19	–224 ± 4	30 ± 6	146 ± 33

$\Delta G°_{ion,Na+}$ = 89.6 kcal mol^{-1} (4)
$\Delta H°_{ion,Na+}$ = 97.3 kcal mol^{-1} (4)
$\Delta G°_{ion,K+}$ = 72.6 kcal mol^{-1} (4)
$\Delta H°_{ion,K+}$ = 77.4 kcal mol^{-1} (4)
$\Delta G°_{hyd} = \Delta C°_P \cdot 80(\pm 10)$K;(5) $\Delta C°_P$ is the experimentally determined value, (see Tables S1 and S2).
$\Delta G°_{int} = \Delta H° - \Delta H°_{ion}$
$\Delta G°_{rt} = -T\Delta S°_{rt}$; $T\Delta S°_{rt}$ = −15 kcal mol^{-1} (6)
$\Delta G°_{conf} = \Delta G° - \Delta G°_{solv} - \Delta G°_{int} - \Delta G°_{rt}$; $\Delta G°$ is the experimentally determined value, (see Tables S1 and S2).
The errors of $\Delta G°$ contributions (Eq. 4 – main text) were calculated combining the errors of experimental quantities ($\Delta G°$, $\Delta H°$, $\Delta C°_P$; global model analysis) and errors reported in the literature ($\Delta G°_{ion}$, $\Delta G°_{hyd}$, $\Delta G°_{rt}$) (4,5,6).

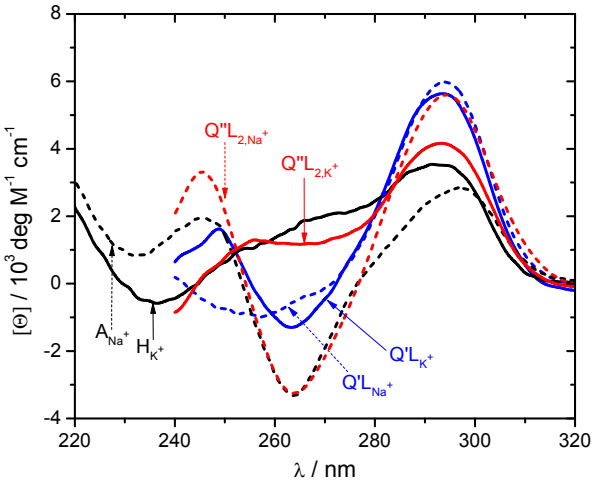

FIGURE S9 CD spectra corresponding to Tel22 antiparallel (A_{Na}+) and hybrid (H_K+) quadruplex structures and complexes with one (Q'L) and two bound ligands (Q''L_2) at 25 °C in the presence of 100 mM K^+ (full lines) or Na^+ (dashed lines) ions and ligand 360A-Br. CD spectra of the complexes were calculated by deconvolution of the measured spectra based on model-predicted populations of species (Figs. S3, S6 and S7) and spectra of Q (A_{Na}+ or H_K+) and I (I_{Na}+ or I_K+) form.

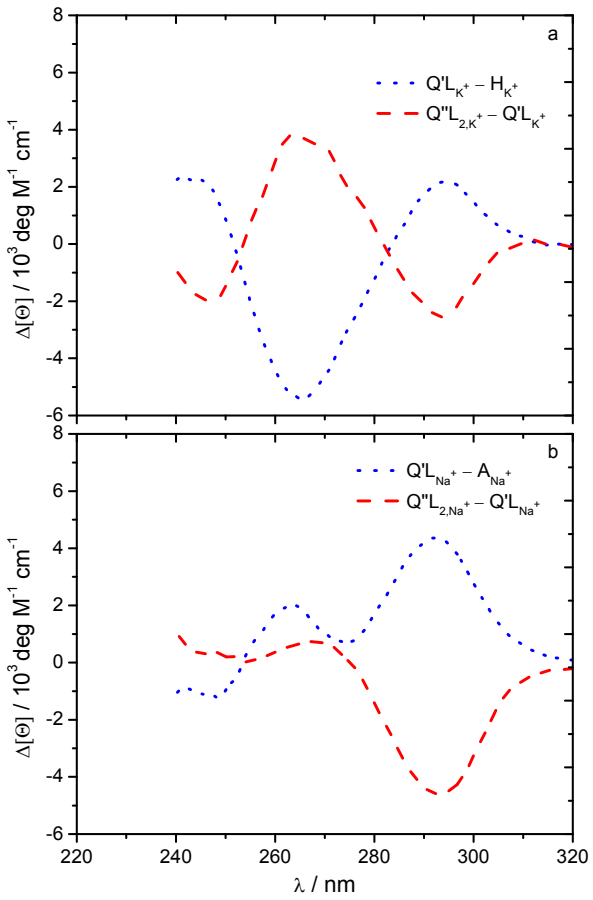

FIGURE S10 Changes of CD spectra upon ligation. Dotted lines represent differences between CD spectra of the complex with one bound ligand molecule (Phen-DC3) and ligand free quadruplex in 100 mM K^+ ($Q'L_{K}+ - H_{K}+$; panel a) and in 100 mM Na^+ ($Q'L_{Na}+ - A_{Na}+$; panel b). Dashed lines represent differences between CD spectra of the complex with two bound ligand molecules and complex with one bound ligand in 100 mM K^+ ($Q''L_{2,K}+ - Q'L_{K}+$; panel a) and in 100 mM Na^+ ($Q''L_{2,Na}+ - Q'L_{Na}+$; panel b).

Correlation between Adjustable Parameters

Representative correlation matrixes are presented in Tables S4 and S5. Correlation matrix corresponding to the global model analysis of DSC and CD data (folding/unfolding of Tel22 in presence of ions, Table S4) shows high correlation between parameters $\Delta G^{o}_{QI(T_0,X^+)}$ - Δn_{QI} (> 0.90) while in the case of global model analysis of ITC and CD data (ligand binding on Tel22, Table S5) between parameters $\Delta G^{o}_{Q''L_2(T_0,X^+)}$ - $\Delta n_{Q'L}$ and $\Delta[\Theta]_{QI}$ - $\Delta[\Theta]_{Q'L}$. Therefore, the physical meaning of these adjustable parameters may be questionable. For this reason we performed the fitting procedure starting with significantly different initial values of the adjustable parameters. The obtained best fit values of all parameters were always within the error margins presented in Table S1 and S2. Moreover, poorer agreement between the model function and experimental data was observed when highly correlated $\Delta G^{o}_{QI(T_0,X^+)}$ and Δn_{QI} or $\Delta G^{o}_{Q''L_2(T_0,X^+)}$ and $\Delta n_{Q'L}$ were varied simultaneously (at fixed best-fit values of other parameters) for the ±error($\Delta G^{o}_{QI(T_0,X^+)}$) and ±error(Δn_{QI}) or ±error($\Delta G^{o}_{Q''L_2(T_0,X^+)}$) and ±error($\Delta n_{Q'L}$) reported in Tables S1 and S2. This suggests that the parameters analyzed above are reliable within the estimated error margins (Tables S4 and S5). On the other hand, the observed high correlation between spectroscopic parameters $\Delta[\Theta]_{QI}$ and $\Delta[\Theta]_{Q'L}$ has no effect on the best-fit values of thermodynamic quantities.

TABLE S4 Correlation matrix corresponding to the global model analysis of the DSC and CD (Eqs. 3, 4) folding/unfolding data of Tel22 measured at different K^+ concentrations. Highly correlated adjustable parameters are marked red.

	$\Delta G^{o}_{QI(T_0,X^+)}$	$\Delta H^{o}_{IU(T_0)}$	Δn_{QI}	$\Delta G^{o}_{IU(T_0,X^+)}$	$\Delta H^{o}_{IU(T_0)}$	$\Delta C^{o}_{P,IU}$	Δn_{IU}	Δf_{QI}
$\Delta G^{o}_{QI(T_0,X^+)}$	1.00							
$\Delta H^{o}_{IU(T_0)}$	0.39	1.00						
Δn_{QI}	0.92	0.14	1.00					
$\Delta G^{o}_{IU(T_0,X^+)}$	0.43	-0.09	0.64	1.00				
$\Delta H^{o}_{IU(T_0)}$	0.54	-0.07	0.72	0.84	1.00			
$\Delta C^{o}_{P,IU}$	-0.61	0.04	-0.74	-0.79	-0.88	1.00		
Δn_{IU}	-0.17	-0.20	-0.04	0.40	0.10	-0.02	1.00	
Δf_{QI}	0.00	0.00	0.00	0.00	0.00	0.00	0.00	1.00

TABLE S5 Correlation matrix corresponding to the global model analysis of the ITC and CD (Eqs. 5,9) Phen-DC3 binding data on Tel22 measured at different *T* and K^+ concentrations. Highly correlated adjustable parameters are marked red.

	$\Delta G^{o}_{Q'L(T_0,X^+)}$	$\Delta H^{o}_{Q'L(T_0)}$	$\Delta G^{o}_{Q''L_2(T_0,X^+)}$	$\Delta H^{o}_{Q''L_2(T_0)}$	$\Delta C^{o}_{P,Q'L}$	$\Delta n_{Q'L}$	$\Delta[\Theta]_{QI}$	$\Delta[\Theta]_{Q'L}$	$\Delta[\Theta]_{Q''L_2}$
$\Delta G^{o}_{Q'L(T_0,X^+)}$	1.00								
$\Delta H^{o}_{Q'L(T_0)}$	-0.35	1.00							
$\Delta G^{o}_{Q''L_2(T_0,X^+)}$	0.80	0.10	1.00						
$\Delta H^{o}_{Q''L_2(T_0)}$	0.07	-0.66	-0.27	1.00					
$\Delta C^{o}_{P,Q'L}$	-0.04	0.14	0.07	0.33	1.00				
$\Delta n_{Q'L}$	0.88	-0.04	0.93	0.00	0.23	1.00			
$\Delta[\Theta]_{QI}$	0.00	0.00	0.00	0.00	0.00	0.00	1.00		
$\Delta[\Theta]_{Q'L}$	0.00	0.00	0.00	0.00	0.00	0.00	-0.94	1.00	
$\Delta[\Theta]_{Q''L_2}$	0.00	0.00	0.00	0.00	0.00	0.00	0.57	-0.78	1.00

PAGE Electrophoresis

DNA dissolved in the buffer-3%DMSO solution containing Na^+ or K^+ ions was mixed with an appropriate amount of ligand in the same buffer-3% DMSO solution to achieve 40 μM DNA solution and the desired DNA/ligand molar ratio *r*. 10 μL of these samples were mixed with 3 μL of 40 % (w/v) sucrose solution and then 10 μL of such modified sample solutions were loaded onto a 22 (w/v) polyacrylamide gel and subjected to a constant voltage of 110 V for 3.5 h. The running TBE buffer, pH = 8.2, contained 0.09 M Tris, 0.09 boric acid and 1 mM EDTA. Electrophoresis cell was placed in a water bath at 25 °C. After the electrophoresis, the gels were photographed under UV light using G-box (Syngene, Cambridge, U.K.).

PAGE mobility patterns show that ligand binding to Tel22 G-quadruplex appears to be a reversible process since the band intensity of the complex and ligand-free DNA changes with *r* ($r = c_{DNA}/c_{L,tot}$). In the case of irreversible binding process the band intensity of the complex would not be a function of *r*. The intensity of the observed mobility patterns is consistent with the calculated model-based fractions of species. PAGE does not distinguish between Q'L and Q''L_2 complexes. Mobility increases in order Q < Q'L ≈ Q''L_2 and is the same in the presence of Na^+ or K^+ ions suggesting similar structure of complexes formed in the presence of K^+ and Na^+ ions. Additional experiments were performed to test reliability of the presented PAGE results. In these experiments polyacrylamide gel itself contained 100 mM salt solution or ligand of different concentrations. The additional experiments gave results that are identical to those presented in Fig. S11.

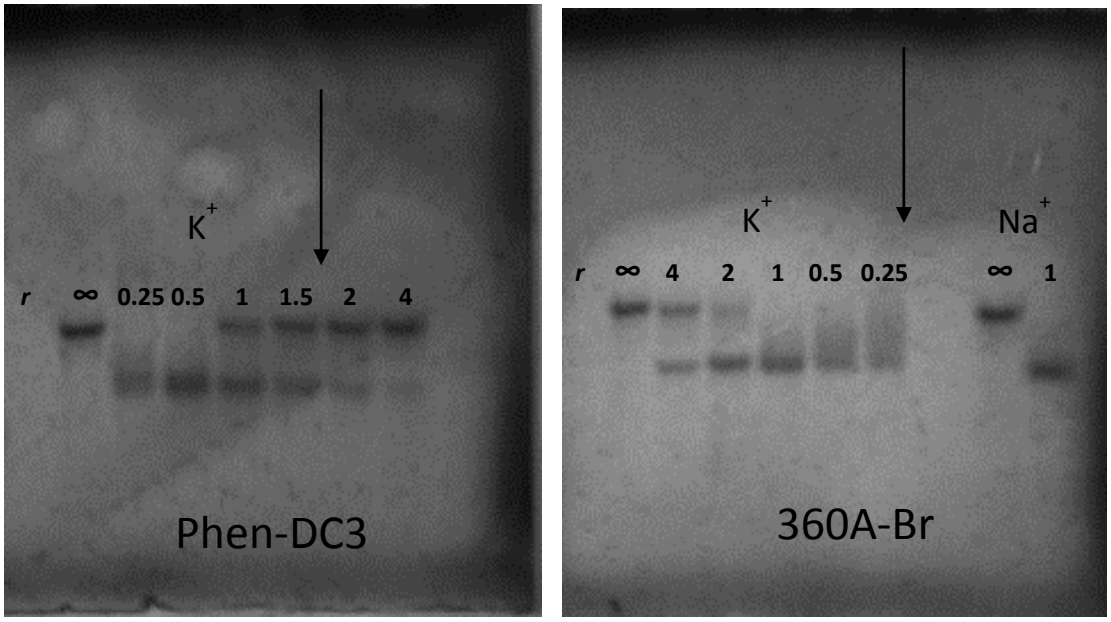

FIGURE S11 Results of PAGE electrophoresis performed at 25°C and 100 mM Na^+ or K^+. *r* is defined as DNA/ligand molar ratio.

REFERENCES

1. Bončina, M., J. Lah, I. Prislan, G. Vesnaver. 2012. Energetic basis of human telomeric DNA folding into G-quadruplex structures. *J. Am. Chem. Soc*. 134:9657-9663.
2. Luque, I., E. Freire. 2002. Structural parameterization of the binding enthalpy of small ligands. *Proteins*, 49:181-190.
3. Ciolkowski, M.L., M.M. Fang, M.E. Lund. 2002. A surface plasmon resonance method for detecting multiple modes of DNA-ligand interactions. *J. Pharm. Biomed. Anal*. 22:1037-1045.
4. Marcus, Y.A. 1986. *Ion solvation*; John Wiley & Sons Ltd.
5. Baldwin, R.L. 1986. Temperature dependence of the hydrophobic interaction in protein folding. *Proc. Natl. Acad. Sci. USA*. 83:8069-8072.
6. Finkelstein, A. V., J. Janin. 1989. The price of lost freedom - entropy of bimolecular complex-formation. *Protein Eng.* 3:1-3.